Universiteit
Leiden
The Netherlands

Delineating the DNA damage response using systems biology approaches

Stechow, L. von

Citation

Stechow, L. von. (2013, June 20). *Delineating the DNA damage response using systems biology approaches*. Retrieved from https://hdl.handle.net/1887/20983

Version:	Corrected Publisher's Version
License:	Licence agreement concerning inclusion of doctoral thesis in the Institutional Repository of the University of Leiden
Downloaded from:	https://hdl.handle.net/1887/20983

Note: To cite this publication please use the final published version (if applicable).

Cover Page

Universiteit Leiden

The handle http://hdl.handle.net/1887/20983 holds various files of this Leiden University dissertation.

Author: Stechow, Louise von
Title: Delineating the DNA damage response using systems biology approaches
Issue Date: 2013-06-20

THE E3 LIGASE ARIH1 PROTECTS AGAINST GENOTOXIC STRESS BY INITIATING A 4EHP-MEDIATED mRNA TRANSLATION ARREST

MANUSCRIPT SUBMITTED

Louise von Stechow, Dimitris Typas, Jordi Carreras Puigvert, Laurens Oort, Ramakrishnaiah Siddappa, Alex Pines, Harry Vrieling, Bob van de Water, Leon HF Mullenders, and Erik HJ Danen

ABSTRACT

In an RNAi screen for (de)ubiquitinases and sumoylases modulating the apoptotic response of embryonic stem (ES) cells to DNA damage, we identify the E3 ubiquitin ligase/ ISGylase, Ariadne homologue 1 (ARIH1). Silencing ARIH1 sensitizes ES and cancer cells to genotoxic compounds and γ-irradiation, irrespective of their p53- or caspase-3 status. DNA damage-induced ATM signaling attenuates ARIH1 proteasomal degradation and the accumulated ARIH1 associates with 4ehp, a competitive inhibitor of the translation initiation factor eIF4E, which undergoes increased ubiquitination upon DNA damage. Genotoxic stress leads to concentration of ARIH1 at ribosomes and triggers 4ehp translocation to the 5' mRNA-cap as well as mRNA translation arrest, in an ARIH1-dependent manner. Finally, restoration of DNA damage-induced translation arrest in ARIH1-depleted cells by an eiF2α dephosphorylation-inhibitor reinstates resistance to genotoxic stress. These findings identify ARIH1 as a mediator of DNA-damage-induced translation arrest that protects stem and cancer cells against genotoxic stress.

INTRODUCTION

DNA damage leads to acute toxicity and the accumulation of mutations and chromosomal instability, potentially resulting in malignant transformation [1; 2]. To counteract these deleterious effects of DNA damage the cell is equipped with a highly complex signaling response termed the DNA damage response (DDR). The DDR activates effector components involved in protective pathways including DNA damage repair, cell cycle arrest, transcription, chromatin remodeling and cell death. In tandem with phosphorylation-mediated signaling, which is largely executed by the PI3Kl like kinases ATM, ATR and DNA-PK, the checkpoint kinases Chk1 and Chk2, and members of the MAPK family [3; 4], protein modifications by ubiquitin and ubiquitin-like moieties are crucial at all levels of the DDR [5].

The ubiquitination machinery can form various, differentially interpreted tags, including both degradative (K48, K11 linked chains) and non degradative (monoubiquitination, K63 linked chains) signals [6]. Furthermore, a growing family of ubiquitin-like modifications such as SUMO, Nedd8 and ISG15 has been identified, mostly providing non-degradative signals. Multiple enzymes are shared between the ubiquitination, sumoylation, and ISGylation systems [7; 8; 9]. Ubiquitin-mediated signaling is vital to many cellular processes, including the response to DNA damage. Recognition and processing of double strand breaks (DSBs) and intrastrand crosslinks, polymerase switching during translesion synthesis (TLS), nucleotide excision repair, and p53 stability are all regulated by ubiquitination [5; 10; 11]. More recently, ISGylation has been implicated in the DDR: ATM-mediated down modulation of the ISG system can serve as a mechanism to enhance ubiquitination-mediated protein turnover after DNA damage [12].

Ubiquitin and ubiquitin-like modifications occur through three enzymatic steps; commencing with an E1 activating enzyme, which forms a thioester bond to the ubiquitin protein. Subsequently the charged ubiquitin monomer is relayed to an E2 enzyme, that conjugates the ubiquitin molecule to its target protein, with the aid of an E3 ubiquitin ligase [13]. While there are only a few E1 and E2 enzymes, a large number of E3 ubiquitin ligases dictates substrate specificity and ensures substrate diversity of the ubiquitin system. There are two E3 ubiquitin ligase families. The ligase in RING ubiquitinases functions as an adaptor protein between the E2 enzyme and the substrate protein, facilitating transfer of the ubiquitin to the target protein. In HECT ubiquitinases, the ubiquitin is first conferred to a conserved residue within the HECT domain and then added to the substrate protein [14]. Recently, ubiquitin ligases of the Parkin family including Parkin and human homologue of Ariadne1 (ARIH1; HHARI) have been demonstrated to be hybrids between HECT and RING domain ubiquitin ligases [15].

After DNA damage, ongoing transcription and translation have to be adjusted to allow execution of stress-specific programs, save energy, accomplish DNA repair and avoid the transcription and subsequent translation of potentially mutated genetic material [16]. Genotoxic stress has been shown to induce a block in protein synthesis [17; 18; 19]. Eukaryotic mRNAs are mostly recruited to the ribosome through their

5' 7-methylguanosine cap [20]. The rate-limiting step of eukaryotic cap-dependent translation initiation is the binding of the translation initiation factor eIF4F to the mRNA 5'cap structure. eIF4F is composed of the cap-binding protein eIF4E, the RNA helicase eIF4A and the scaffold protein eIF4G [21; 22].

Here, we describe the identification of the Parkin family E3 ubiquitin ligase, ARIH1 in an RNAi screen for modulators of chemosensitivity. We show that ARIH1 levels and cellular localization are regulated in response to DNA damage. In turn, ARIH1 protects stem- and cancer cells against genotoxic compounds and γ-irradiation through a 4ehp-mediated mRNA translation arrest.

RESULTS

A ubiquitination RNAi screen identifies cisplatin response modulators

We performed an siRNA-based screen using the Dharmacon ubiquitination Smartpool library and custom made Smartpool libraries targeting all known cellular deubiquitinases (DUBs), sumoylases, and desumoylases (Table S1). Mouse embryonic stem (ES) cells that display a robust apoptotic response to genotoxic compounds, including cisplatin (Fig S1), were treated with 10 μM cisplatin or vehicle and cell viability was monitored after 24 h. 50 Smartpools were identified that met selection criteria [Z-score +/- 1.5; p-value > 0.05] (Fig 1A; Table S2). As controls, we included siRNA Smartpools targeting Kif11, expected to induce cell killing due to mitotic spindle defects or targeting p53, expected to protect ES cells against cisplatin-induced killing. In all experimental plates, siKif11 resulted in ~90% reduction in viability and sip53 protected against cisplatin-induced loss of viability (Fig S2A). As a quality measurement Z'-factors were calculated based on siLamin (negative control) and sip53. The average of calculated Z'-factors was 0.45, indicating a good signal to noise ratio and reproducibility of the screens (Fig S2B). To exclude off target effects, selected Smartpools entered a deconvolution screen where 27/50 hits could be confirmed with at least 2/4 sequences reproducing the effect of the Smartpool (Fig 1B,C, Table S3).

The 27 confirmed hits included six DUBs, one E1 ubiquitin-activating enzyme, Ube1x, one E2 ubiquitin-conjugating enzyme, UBE2D3, as well as 12 siRNAs targeting E3 ubiquitin ligases. Moreover, we identified seven siRNAs targeting proteins with no described ubiquitinase function that were included in the ThermoFischer "ubiquitination library" presumably based on the presence of predicted domains associated with ubiquitinase function, including RING, SOCS, or SPRY (see discussion). The knockdown of the E1 ubiquitin enzyme Ube1x (Uba), which has recently been shown to be a crucial E1 enzyme in the DDR following ionizing radiation and replication stress 23, resulted in a particularly strong reduction of viability (Fig 1C).

Enrichment of p53-modyfiers and DNA repair regulators

A large proportion of the identified hits have been previously established to control the levels or activity of the transcription factor p53, which acts as a master regulator of the outcome of the DDR in various cell types including ES cells (Fig 1E). Three of the identified DUBs, USP7 (HAUSP), USP4, and USP5 can directly or indirectly influence p53 protein levels [10; 24; 25; 26]. In addition, the E3 ligases Rfwd3, Pirh2 and TOPORS were previously shown to affect p53 stability [10; 27; 28] (Fig 1E; Table S3). Besides p53 regulators we identified several other ubiquitin ligases implicated in DDR-related processes, such as postreplication repair (SHPRH [29], translesion synthesis (Pirh2 [30]), DSB repair (BRCA1 [31]), and the RPA-mediated repair of single strand breaks (Rfwd3 [32]).

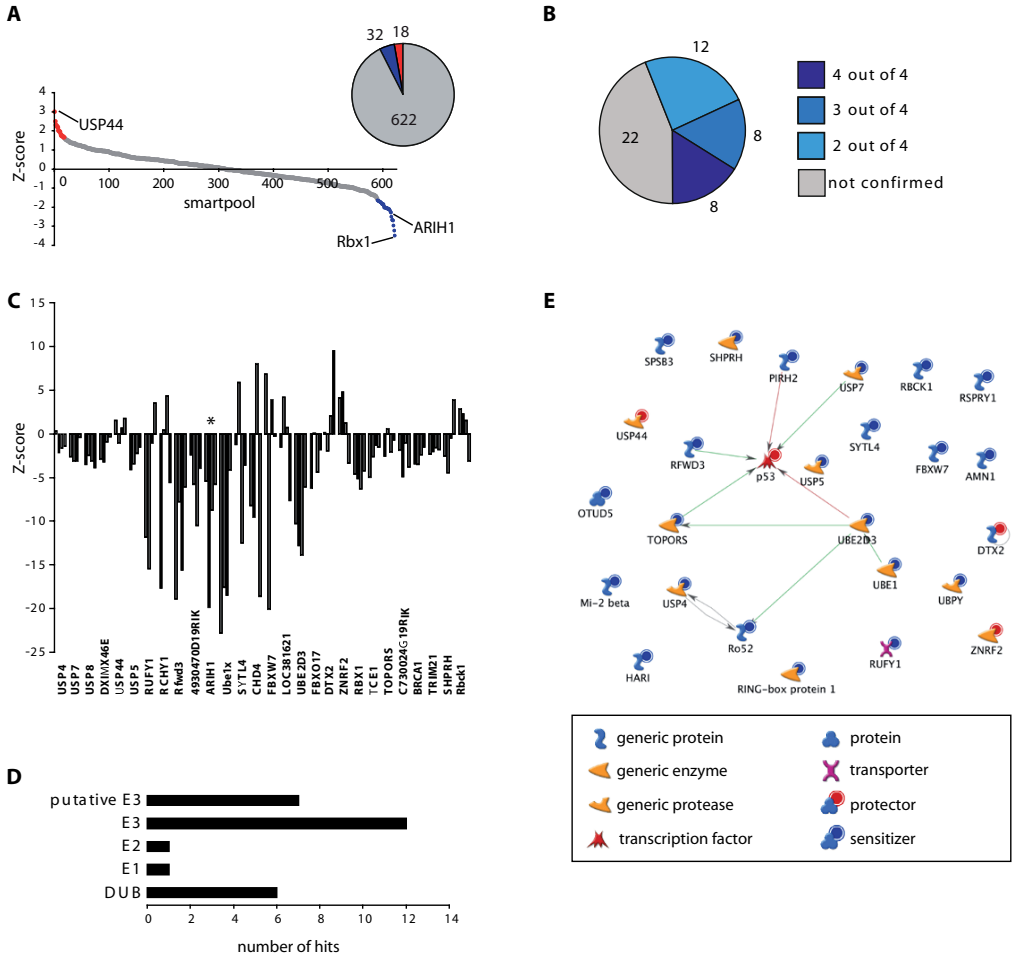

Figure 1. RNAi screen for ubiquitination / sumoylation enzymes identifies cisplatin response modulators. (A) Hits identified in primary screens; protecting siRNA Smartpools in red, sensitizing siRNA Smartpools in blue. (B) Results of deconvolution screen for 50 Smartpools identified in primary screen. (C) Z-scores obtained for 27 confirmed hits in deconvolution screen. Asterisk marks ARIH1 results. (D) Distribution of hits over different gene families as indicated. (E) Metacore-predicted network derived form screen hits; interactions with p53 are indicated. Red circles, protecting siRNAs; blue circles, sensitizing siRNAs.

Accordingly, Metacore-based pathway analysis of the 27 confirmed ubiquitination-screen hits identified DNA damage signaling and repair processes to be prominently enriched (Fig S3).

Silencing ARIH1 sensitizes to genotoxic stress

One of the strongest hits in the screen was the Parkin family ubiquitin ligase Ariadne homologue 1 (ARIH1) [33]. The ARIH1 Smartpool and all four of the individual sequences tested in the deconvolution experiments, significantly sensitized ES cells to cisplatin-induced loss-of-viability (Fig 1A,C; Table S3). In order to examine if the effect of silencing ARIH1 was specific for the type of induced (genotoxic) stress, the effect of ARIH1 knockdown in ES cells was examined after treatment with various genotoxic and non-genotoxic compounds. Compounds were used at a dose, which induces comparable loss-of-viability at 24 h (Fig 2A). Notably, knockdown of ARIH1 using the Smartpool or either of three individual siRNAs did not significantly affect ES cell viability under control conditions (Fig 2B,C).

Similar to its effect on cisplatin-sensitivity, silencing ARIH1 significantly sensitized ES cells to all tested genotoxic drugs, including the topoisomerase inhibitors etoposide and doxorubicin and the DNA crosslinking compound mitomycin C (Fig 2B,C). In contrast, knockdown of ARIH1 did not sensitize ES cells to non-genotoxic agents such as the ER stressor thapsigargin, the oxidative stressor diethyl maleate (DEM), or the microtubule poison vincristine (Fig 2A,C). We also tested the effect of silencing ARIH1 in U2OS p53 wild type human sarcoma cells, which are relatively resistant to cisplatin compared to ES cells. We introduced lentiviral shRNAs targeting ARIH1 and following bulk puromycin selection identified two short hairpins providing ~90% reduction in ARIH1 protein levels (Fig 2D). Basal cell survival was reduced in these knockdown cells when compared to a lentiviral control cell line (Fig 2E) and, analogous to its role in ES cells, silencing ARIH1 significantly sensitized U2OS cells to treatment with 10 or 25 μM cisplatin for 48 h (Fig 2E).

Finally, we tested whether ARIH1 plays a similar role in controling sensitivity to radiation-induced DNA damage. Control and ARIH1-depleted U2OS cells were treated with increasing dosages of cisplatin, ionizing radiation or UV light and colony-forming ability was assessed. Silencing ARIH1 sensitized U2OS cells to cisplatin and γ-irradiation but did not affect the response to UV (Fig 2F-H).

Silencing ARIH1 enhances cell death in a p53- and caspase-3-independent fashion

Since silencing ARIH1 sensitized cells to several genotoxic stressors that lead to the formation of primary and secondary DSBs, we asked if ARIH1 affects the dynamics of DSB repair foci. Formation of γH2AX and 53BP1 foci after treatment with γ–irradiation was similar for shcontrol and shARIH1 U2OS cells. Subsequent foci disappearance, which is associated with repair, was slightly delayed but was similar in control and ARIH1-depleted cells at 24 hours after γ–irradiation (Fig 3A; Fig S4). ARIH1, in contrast to many of the other identified hits (Fig 1E, Table S3), also did not control basal or genotoxic

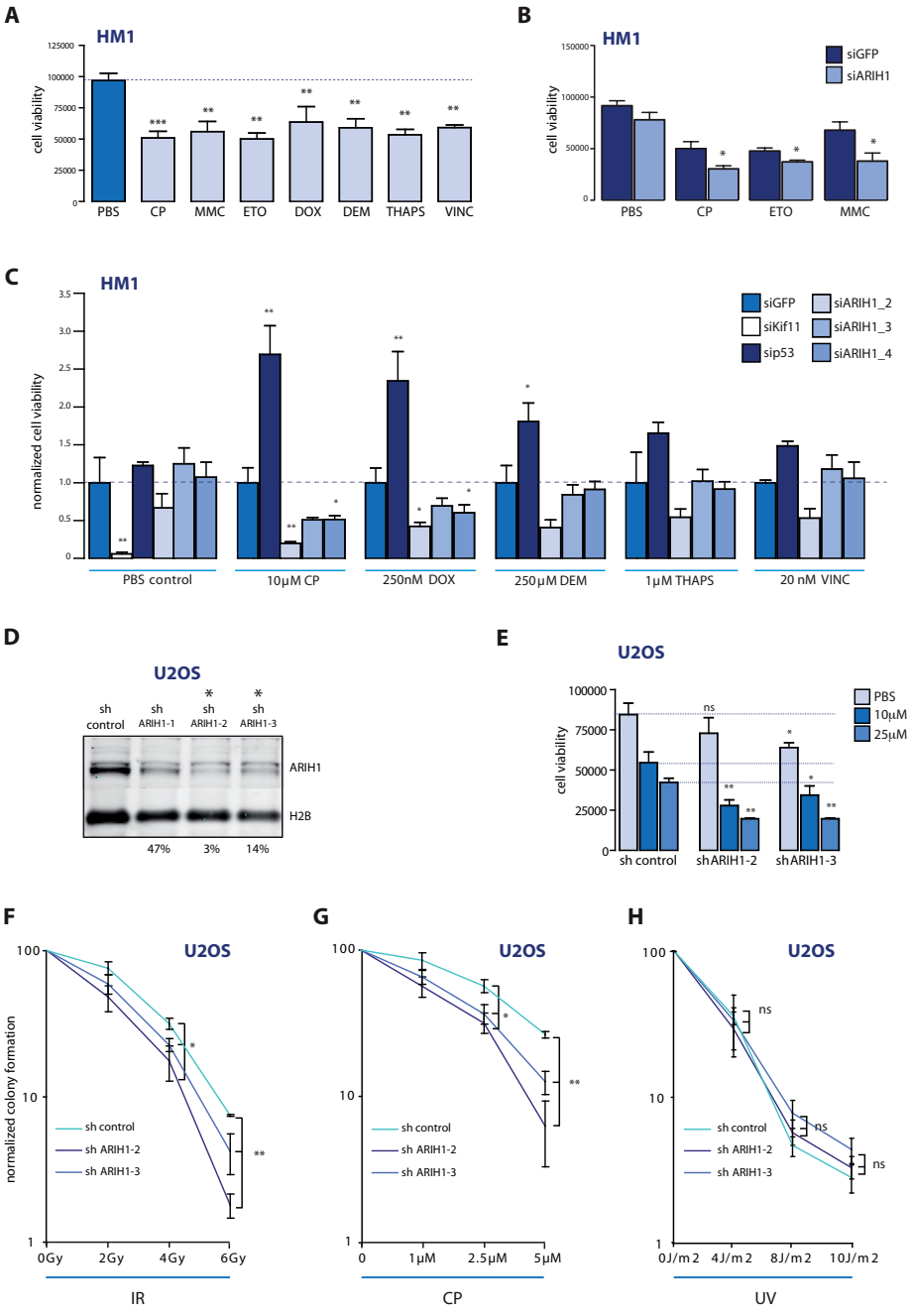

Figure 2. Silencing ARIH1 sensitizes to genotoxic stress. (A) ES cell viability after treatment with 10 μM cisplatin (CP), 10 μg/μl mitomycin C (MMC), 150 nm etoposide (ETO), 250 nM doxorubicin (DOX), 250 μM diethylmaleathe (DEM), 1 μM thapsigargin (THAPS), or 10 nM Vincristine (Vinc). (B) ES cell viability in presence of control or ARIH1 siRNA after treatment with CP, Eto, or MMC. (C) ES cell viability in presence of Kif11-siRNA (only for PBS), GFP-siRNA, p53-siRNA, or 3 individual siRNA sequences targeting ARIH1 after treatment with vehicle control, CP, DOX, DEM, THAPS or VINC (normalized to siGFP). (D) ARIH1 protein levels and H2B loading control in U2OS expressing shcontrol or 3 individual shRNAs targeting ARIH1, followed by bulk puromycin selection. Percentages indicate remaining ARIH1 expression. Asterisks indicate shARIH1 #2 and #3 used in all further experiments. (E) U2OS cell viability in shcontrol or 2 individual shARIH1 cell lines after treatment with vehicle (PBS) or 10 or 25 μM CP for 48 h. (F, G, H) Colony formation capacity in shcontrol or shARIH1-2 and -3 U2OS cell lines after treatment with γ–irradiation (IR), CP, or UV-radiation at indicated exposure conditions. *p<0.05; **p<0.01.

stress-induced p53 stability in ES cells or U2OS cells (Fig 3B,C). In agreement, silencing ARIH1 sensitized the p53-deficient non-small-cell lung cancer cell line H1299 [34] and the p53 mutant mouse breast cancer cell line 4T1, to cisplatin (Fig 3D-G). DNA damage can trigger a p53-dependent or independent cell cycle arrest. In ES cells, ARIH1 knockdown did not significantly alter cell cycle distribution or cisplatin-induced S/G2 phase arrest (Fig 3H).

These data suggested that ARIH1 is mainly implicated in maintaining viability while the cell cycle is arrested and repair is ongoing. Indeed, silencing ARIH1 increased the subG1/G0 fraction after treatment with cisplatin (Fig 3I). This effect of ARIH1 was not restricted to capase-3-mediated apoptosis, since transient or stable silencing of ARIH1 also sensitized the caspase-3 deficient human breast cancer cell line MCF7 (Fig 3J-L). Notably, as observed in ES cells ARIH1 knockdown did not affect basal cell cycle distribution or cisplatin-induced cell cycle arrest in MCF7 (Fig 3M, Fig S4).

In summary, ARIH1-depleted cells respond to DSBs by normal levels of DDR foci formation and induction of cell cycle arrest. In spite of this, cell survival following DNA damage is severely compromised in the absence of ARIH1 and this increased sensitivity is independent of p53 or caspase-3-mediated apoptosis.

Cisplatin induces 4ehp cap-binding and translation arrest in an ARIH1-dependent manner

We tested if DNA damage may trigger the expression of ARIH1. ARIH1 protein levels were enhanced following cisplatin treatment in U2OS cells (Fig 4A). This could not be explained by enhanced mRNA levels, indicating that genotoxic stress triggered increased synthesis or enhanced stability of the ARIH1 protein (Fig 4B). Treatment with the proteasome inhibitor, MG132 enhanced basal ARIH1 levels and prevented cisplatin-induced ARIH1 accumulation (Fig 4C). Moreover, inhibition of ATM, a central kinase within the DDR signaling network, blocked cisplatin-induced ARIH1 accumulation indicating that DNA-damage caused ATM-mediated attenuation of proteasomal degradation of ARIH1.

In response to DNA damage, ongoing cellular activities are suppressed while stress programs and DNA repair processes are activated. One typical response is the acute inhibition of protein synthesis through alterations of the cap-dependent translation initiation complex [35]. This can be achieved in several ways, including recruitment of 4ehp (eIF4E2), a competitive inhibitor of the canonical cap-binding translation initiation factor, eIF4E [20]. In contrast to eIF4E, 4ehp cannot bind the structural component eIF4G that is required for ribosome recruitment and subsequent mRNA translation. Although ARIH1 can act as an E3 ubiquitin ligase for 4ehp [36] more recently it has been established that ARIH1 can ISGylate 4ehp thus enhancing its affinity for the mRNA cap structure and replacing eIF4E [37]. Co-immunoprecipitations in U2OS cells showed that the increased levels of ARIH1 in cisplatin-treated cells led to ARIH1 association with 4ehp (Fig 4D). We analyzed cisplatin-induced post translational modification of wild type 4ehp and a Lys[K121/130/134/222R]-mutant that cannot be ISGylated [37].

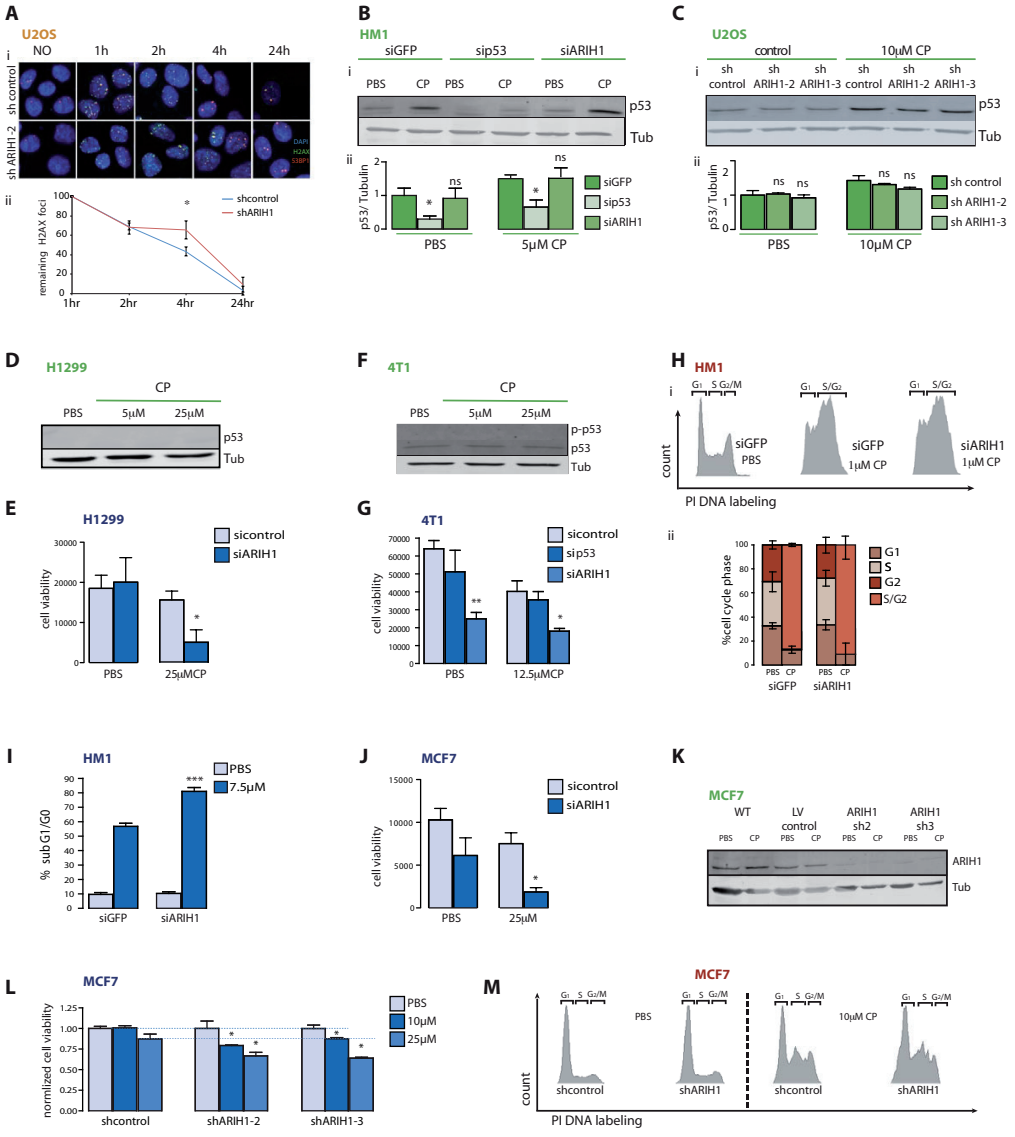

Figure 3. Silencing ARIH1 enhances cancer cell death in response to genotoxic stress in a p53 & caspase-3 independent manner. (A) i) Immunostaining for γH2AX (green), 53BP1 (red), and DAPI (blue) in U2OS cells expressing indicated shRNAs under non-irradiated conditions (NO) or after treatment with γ-irradiation for indicated times. ii) Quantification of remaining γH2AX foci at indicated timepoints derived from 3 independent experiments. (B) i) p53 and tubulin control protein levels in ES cells in presence of indicated siRNAs treated with PBS control or 5 μM CP for 8 h. ii) Quantification of Western blot data from i) (n=4). (C) i) p53 and tubulin control protein levels in U2OS cells in presence of control or ARIH1 shRNAs treated with PBS control or 10 μM CP for 16 h. ii) Quantification of Western blot data from i) (n=3). (D) p53 and tubulin control protein levels in p53-deficient H1299 cells treated with indicated concentrations of CP for 24 h. (E) H1299 cell viability under control or siARIH1 conditions after treatment with vehicle control PBS or 25 μM CP for 24 h. (F) WB for p-p53 and p53 in p53-mutant 4T1 cells treated with 5 or 25 μM CP for 12 h. (G) 4T1 cell viability under control, siARIH1, or sip53 conditions after treatment with treated with indicated concentrations of CP for 24 h. (H) i) FACS profiles for HM1 cell cycle content under control, siGFP, or siARIH1 conditions after treatment with control or 1 μM CP. ii) Cell cycle distribution derived from profiles from i) (n=3). (I) Sub-G1/G0 apoptotic fraction of control or siARIH1 ES cells treated with 7.5 μM CP for 24h. (J) MCF7 cell viability under control or siARIH1 conditions after treatment with PBS or 25 μM CP for 48 h. (K) ARIH1 and tubulin control protein levels in MCF7 cells bulk puromycin-sorted for expression of control shRNA or different shRNAs targeting ARIH1. (L) Cell viability for shcontrol and shARIH1-2 and -3 MCF7 cell lines treated for 48 h with PBS or 10 or 25 μM CP. (M) FACS analysis for cell cycle content in shcontrol and shARIH1-2 MCF7 cell lines treated for 24 h with PBS or 10 μM CP. *p<0.05; **p<0.01.

FLAG immunoprecipitation showed two bands of higher molecular weight appearing upon cisplatin treatment (Fig 4E). These corresponded to 4ehp modified either with one ubiquitin molecule (28+7 kD) and to 4ehp modified either with two ubiquitin molecules or with one ISG15 molecule (28+15 kD). These modifications were observed for wild type as well as mutant 4ehp, arguing against ISGylation. Moreover, the [28+15] kD bands were detected by a ubiquitin antibody whereas co-expressed HA-ISG15 did not overlay with these bands, despite the fact that free ISG15 was readily detected in the FLAG immunoprecipitations (Fig 4E).

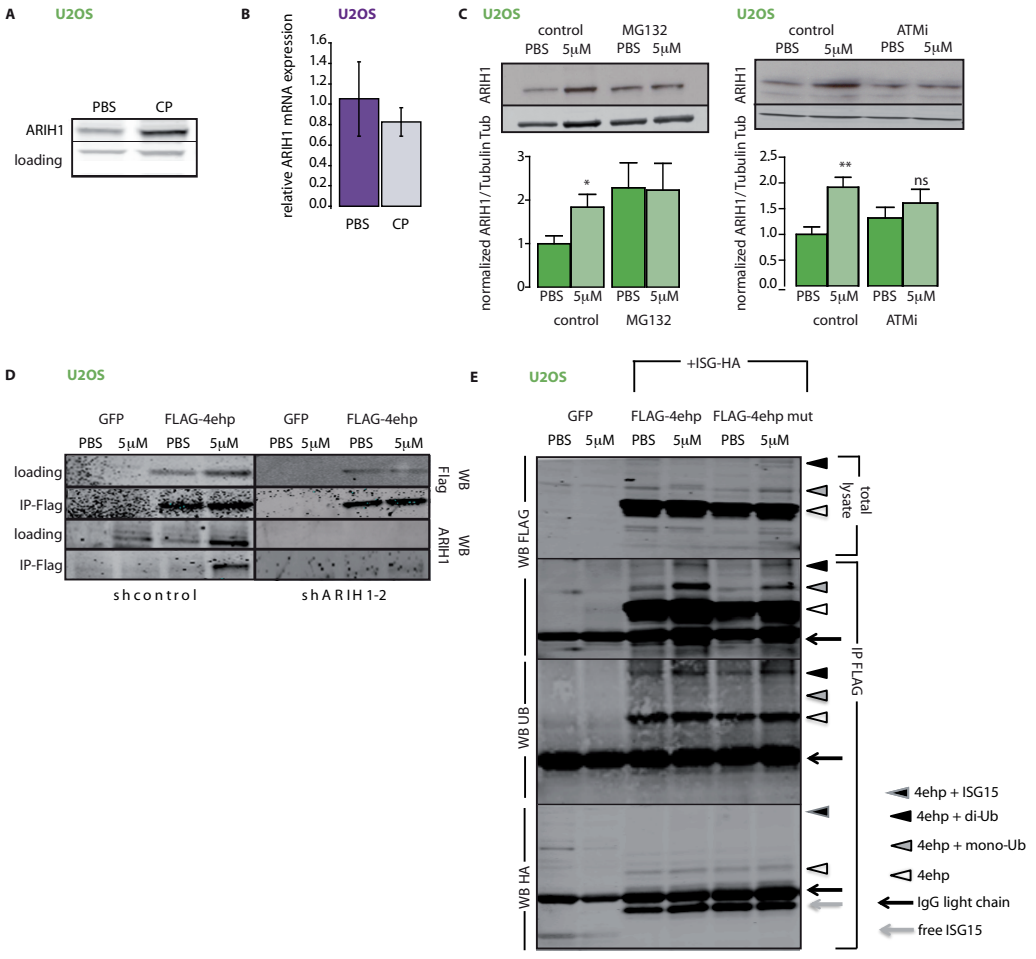

Figure 4. ARIH1 accumulates after DNA damage and interacts with 4ehp. (A) ARIH1 protein levels in U2OS cells treated for 4 h with PBS or 5 μM CP. (B) qPCR analysis of ARIH1 RNA levels, normalized to GAPDH in U2OS cells treated for 4 h with PBS or 5 μM CP. (C) Western blot for ARIH1 and tubulin loading control. For inhibitor treatment, cells were pretreated for 30 min with DMSO vehicle control, 5 μM ATM inhibitor KU-55933 or 10 μM MG132 and subsequently exposed to 5 μM cisplatin or vehicle control for 4 h in the presence of indicated inhibitors. Quantification is representative for 4 independent experiments. (D) FLAG pulldown in shcontrol and shARIH1 U2OS cells transfected with GFP control or FLAG-4ehp plasmid and treated with vehicle control or 5 μM CP for 4 h followed by Western blot for FLAG or ARIH1. (E) FLAG pulldown in U2OS cells transfected with GFP control or FLAG-tagged wid type or Lys[K121/130/134/222R]-mutant 4ehp plasmids and treated with PBS control or 5 μM cisplatin for 4 h. Western blot with indicated antibodies (left) is shown. Arrows and arrowheads are explained in legend.

These results suggested that 4ehp is ubiquitinated, rather than ISGylated after genotoxic stress. ARIH1-dependent ISGylation has been reported to regulate 4ehp association with the 5'cap but ARIH1-mediated ubiquitination of 4ehp, although being described, is not known to affect this process. We used 5'cap-pulldown assays to investigate whether cisplatin treatment caused 4ehp translocation to the mRNA cap. Indeed, 4ehp binding to the mRNA cap was induced in response to cisplatin in U2OS, MCF7, as well as ES cells (Fig 5A-D). Importantly, this response was disturbed in the absence of ARIH1.
Basal 4ehp cap-binding was slightly enhanced in MCF7 and ES cells but importantly,

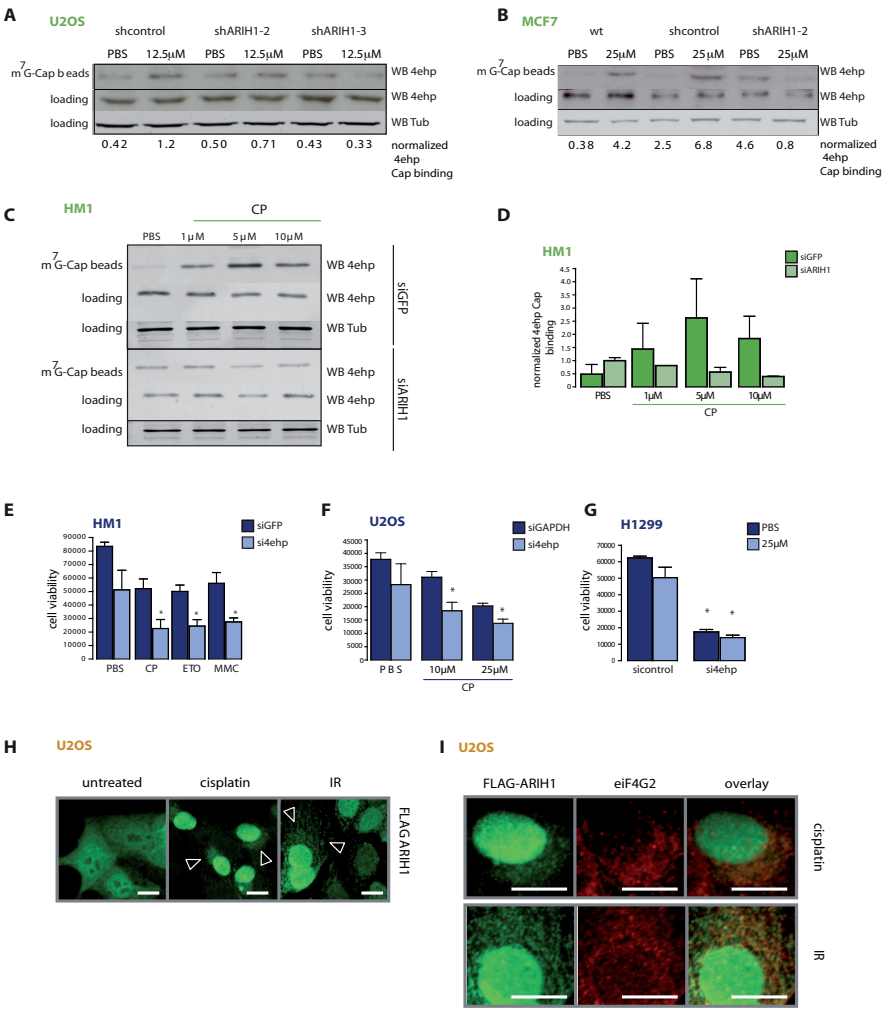

Figure 5. ARIH1 mediates DNA damage-induced Cap binding of 4EHP. (A-C) m^{7}G-Cap pulldown from control and ARIH1-silenced U2OS (A), MCF7 (B) or ES cells (C) treated with vehicle control or indicated concentrations CP followed by Western blot for 4ehp or tubulin control. Numbers at the bottom indicate Cap-associated 4ehp levels relative to total 4ehp. (D) Quantification of m^{7}G-Cap-bound 4ehp in control (n=4) and siARIH1 (n=2) ES cells. (E) ES cell viability under sicontrol or si4ehp conditions after treatment with PBS, 10 μM CP, 150 nm Eto, 10 μg/μl MMC for 24 h. (F) U2OS cell viability under sicontrol (siGAPDH) or si4ehp conditions after treatment with PBS, 10 or 25 μM CP. (G) H1299 cell viability under sicontrol or si4ehp conditions after treatment with PBS or 25 μM CP. (H) FLAG-ARIH1 localization before or after treatment with 5 μM cisplatin for 4 h or 4 h after treatment with 2 Gy γIR. Arrowheads indicate regions of perinuclear accumulation. (I) Higher magnification of perinuclear staining for FLAG-ARIH1 (green), ribosomal marker eiF4G2 (red) staining and overlay after CP treatment or irradiation. *p<0.05; **p<0.01.

cisplatin-induced 4ehp:cap association was abrogated in U2OS, MCF7, and ES cells when ARIH1 was depleted (Fig 5A-D). Subsequently, to test if 4ehp:cap association represents an ARIH1-regulated pathway that could explain the protective role of ARIH1, 4ehp itself was silenced. In line with such a mechanism, ES cells, U2OS cells, as well as p53-deficient H1299 cells were sensitized to genotoxic compounds following 4ehp silencing (Fig 5E-G; Fig S5).

Altogether, these findings indicated that the ability of ARIH1 to protect against genotoxic stress-induced cell death involved 4ehp-mediated translation inhibition at the 5'cap. We performed immunostainings to assess subcellular localization of ARIH1 in response to genotoxic stress. Whereas in untreated U2OS cells ARIH1 was diffusely present in the cytoplasm and nucleus, treatment with cisplatin or γ-IR caused concentration of ARIH1 in the nucleus as well as in perinuclear regions (Fig 5H). In good agreement with a role for ARIH1 in 4ehp-mediated translation arrest, co-staining with a ribosomal marker, eIF4G2 identified these perinuclear regions as ribosomes (Fig 5I).

We next investigated whether the identification of ARIH1 as a mediator of DNA damage-induced 4ehp association with the mRNA cap pointed to a role for ARIH1 in DNA damage-induced translation arrest. Click-iT® metabolic labeling showed that cisplatin treatment caused a strong translation block in U2OS cells at 2 h post-treatment while at later timepoints (4, 8 h) a more modest suppression of translation was maintained (Fig 6A). In line with a critical role for ARIH1 in mediating this arrest, two independent shARIH1 lines failed to arrest translation in response to cisplatin while a cyclohexamide-induced translation block was intact (Fig 6A). Co-treatment with salubrinal, an inhibitor of eIF2α dephosphorylation that inhibits translation under stressed conditions, could restore the translation block at 2 h cisplatin treatment in ARIH1 knockdown cells (Fig 6B). Finally, consistent with a protective function of the ARIH1-controled translation arrest, salubrinal also restored cell viability in cisplatin-treated ARIH1-silenced U2OS cells, ES cells and MCF7 cells (Fig 6C-E).

Altogether, these findings indicate that DNA damage-induced increase in ARIH1 protein levels lead to association of ARIH1 with 4ehp. This causes 4ehp recruitment to the mRNA cap where it replaces eIF4E. The resulting mRNA translation arrest acts cytoprotective: ARIH1 or 4ehp depletion sensitizes cells to genotoxic stress while reestablishing the translation block with salubrinal alleviates this effect (Fig 6F).

DISCUSSION

Ubiquitination plays a vital role in the DDR signal transduction cascade. Our RNAi screen targeting the cellular ubiquitination and sumoylation machinery identifies several genes that modulate the response to the chemotherapeutic drug cisplatin. Some of the identified DUBs and E3 ubiquitin ligases have previously been implicated in p53 regulation or DNA repair processes [5]. In addition, the screen identifies genes associated

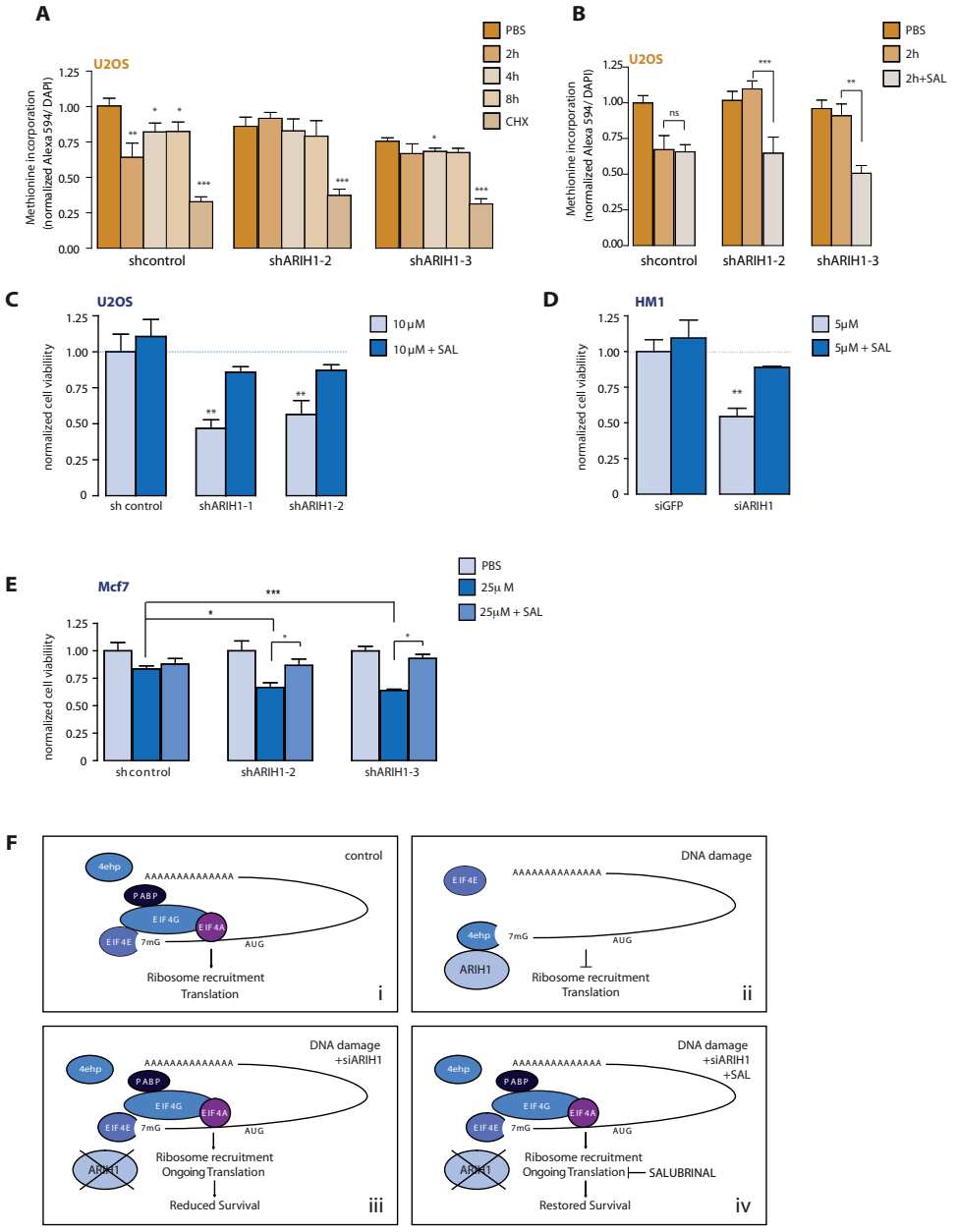

Figure 6. ARIH1 mediates cisplatin-induced mRNA translation arrest. (A) Methionine incorporation in shcontrol and two different shARIH1 U2OS cell lines after treatment with 15 µM CP for 2 h, 4 h or 8 h or cyclohexamide (CHX) for 1 h. Alexa546 signal (reflecting amount of newly synthesized proteins) / number of nuclei (DAPI) is shown, normalized to control in PBS condition is shown. (B) Methionine incorporation in shcontrol and two different shARIH1 U2OS cell lines after treatment with 15 µM CP or co-treatment with 15 µM CP and 2.5 µM salubrinal (SAL) for 2 h is shown. Normalized to Alexa546 fluorescence / nucleus value in PBS for each cell line. (C-E) Cell survival in cells expressing indicated siRNAs or shRNAs after treatment with indicated concentrations of CP in absence or presence of 2.5 µM SAL. C, U2OS 48 h treatment; D, ES cells 24 h treatment; E, MCF7 48 h treatment. (F) Cartoon depicting the role for ARIH1 in regulating sensitivity to genotoxic stress: i) Under non-stressed conditions eIF4E binds to the mRNA Cap and recruits eiF4G and –A driving mRNA translation; ii) upon genotoxic stress ARIH1 accumulates and associates with 4ehp, resulting in recruitment of 4ehp to the Cap where it replaces eIF4E resulting in translation arrest that is cytoprotective; iii) in the absence of ARIH1 (or 4ehp) DNA damage-induced translation arrest does not occur and cell survival is compromised; iv) co-treatment with salubrinal inhibits translation under stressed conditions through inhibition of eIF2α dephosphorylation causing restored translation arrest and survival in the absence of ARIH1 under genotoxic stress.

with cell cycle control or developmental processes (Fig S2). These include Fbxw7, which marks several proto-oncogenes,such as Myc, Jun, cyclin E, and Notch for degradation; and Dtx2, an E3 ligase also proposed to control the Notch signaling pathway [38; 39; 40]. Yet another group of identified hits has been associated with intracellular transport processes, including the DUB USP8, which regulates endosomal sorting of membrane receptors and RUFY and SYTL4, which are involved in Rab-mediated vesicular transport [41; 42; 43]. This suggests that changes in intracellular sorting and recycling might be important for survival after DNA damage.

Notably, some of the hits do not have established (de)ubiquitinase function. On the one hand, this group contains proteins without any domains associated with (de) ubiquitinase activity. These include the Rab-interacting proteins RUFY and SYTL4 that have a FYVE- Zinc finger domain and the Zinc finger-containing chromatin remodeling factor CHD4 [41; 43; 44]. On the other hand, we identify two proteins, TCE1 and Rspry1, characterized by the presence of a SPRY domain. This motif is found in members of the TRIM-family of ubiquitin ligases [45]. In addition, Rspry1 contains a RING domain and TCE1 also harbours a SOCS box domain, which mediates interactions with the Elongin BC complex, an adapter module in E3 ubiquitin ligase complexes [46].

The Parkin family ubiquitin ligase, ARIH1 has not been previously implicated in DDR signaling. Our findings reveal that ARIH1 protects pluripotent stem cells as well as various cancer cells to the toxic effects of ionizing radiation and chemical agents that cause DSB. In absence of ARIH1, the formation of repair foci is unaffected but their clearance is slightly delayed while cell cycle arrest remains intact. Moreover, the cytoprotective role of ARIH1 is also observed in cancer cells lacking a functional p53 or caspase-3 response. Hence, ARIH1 is not required specifically for dampening p53-induced caspase-3-mediated apoptosis. Instead, we find that ARIH1 mediates an mRNA translation arrest in response to DNA damage by binding to 4ehp and stimulating its recruitment to the 5'mRNA Cap.

The obstruction of mRNA translation is an important event in the response to cellular stress and alterations in this regulatory hub have been suggested to be important for resistance of cancer cells to therapy [19; 47]. A well-described mechanism for translation repression is enhanced interaction of the cap-binding protein eIF4E with its negative regulator eIF4-BP1. Under normal conditions this interaction is suppressed by mTOR-mediated phosphorylation of eIF4-BP1 [48]. Alternative eIF4-dependent and independent mechanisms for translation repression have been described [20]. For instance, impaired Met t-RNA recruitment through eif2α Ser51 phosphorylation represents a canonical response to accumulation of improperly folded proteins in the endoplasmic reticulum; the so-called unfolded protein response [49]. Yet another way to arrest mRNA translation is through enhanced 5'mRNA cap-binding of eIF4E2, also known as 4ehp [50]. Our findings implicate this latter mechanism in the DNA damage-induced protein synthesis arrest and provide evidence for an important role for ARIH1 in this step.

4ehp is a eIF4E homologue that has low affinity for binding the cap structures of most mRNAs [51]. The protein has been implicated in the regulation of translation of a

specific subset of mRNAs in *Drosophila* involved in embryonic patterning [52; 53]. ARIH1 can ISGylate 4ehp resulting in increased 5'mRNA cap affinity but it is not known under which conditions ARIH1-mediated ISGylation of 4ehp is induced [37; 54]. Here we demonstrate that in response to DSB-inducing genotoxic stress, ARIH1 protein accumulates and interacts with 4ehp leading to increased recruitment of 4ehp to the 5'mRNA cap. We show that genotoxic stress-induced protein accumulation depends on activity of ATM, a critical kinase in the DDR and that accumulation is most likely mediated by inhibition of proteosomal degradation. Our findings using a non-ISGylatable 4ehp mutant and HA-ISG15 co-immunoprecipitations do not point to 4ehp ISGylation in response to genotoxic stress. Instead, ubiquitination appears to be the predominant 4ehp modification that is enhanced by DNA damage.

Translation arrest is effectuated by 4ehp due to its capacity to act as a competitive inhibitor for eIF4E, which, unlike eIF4E, cannot bind the structural component eIF4G required for ribosome recruitment. In line with this, 4ehp cannot complement eIF4E in gene knockout experiments in yeast [55]. Indeed, the translation block that we observe in cisplatin-treated cells is ARIH1-dependent. Moreover, similar to RNAi targeting ARIH1, depletion of 4ehp sensitizes ES or cancer cells to DNA damage. Our findings do not support the idea that this genotoxic stress-induced arrest in protein synthesis is lost in cancer cells as was described for other eIF4E-dependent routes, such as 4EBP-1 phosphorylation [19]. U2OS cells do arrest and depletion of ARIH1 leads to sensitization of all cancer cell lines tested thus far. Intriguingly, while inhibition of eIF4E cap binding can sensitize cancer cells to different chemotherapeutics [19; 47], our findings indicate that inhibition of the competitive process involving ARIH1 and 4ehp also sensitizes ES cells and different cancer cell lines. Clearly, ongoing 5' cap-mediated translation as well as the ability to temporarily arrest translation in response to DNA damage is required for (cancer) cells to escape genotoxic stress-induced death. Our immunofluorescence experiments indicate that upon genotoxic stress, ARIH1 is concentrated not only in nuclei but also at ribosomes, placing it at the correct location to control this process.

As mentioned above, an alternative route to attenuate protein synthesis is through eiF2α Ser51 phosphorylation and this is typically triggered by an accumulation of misfolded proteins in the ER [49]. This response can be enhanced by salubrinal, an inhibitor of the phosphatase complex that dephosphorylates eIF2α [56]. Interestingly, treatment with salubrinal restores the cisplatin-induced translation arrest as well as survival in ARIH1-depleted cells. This shows that alternative means for attenuating protein synthesis can compensate for the inability to do so through enhanced 4ehp:cap binding. Moreover, it provides further evidence for a model in which the ability of ARIH1 to couple genotoxic stress to attenuation of mRNA translation underlies its cytoprotective role. Finally, restored survival in the presence of salubrinal argues against an important role in this response for enhanced translation of a specific subset of mRNAs, which has also been attributed to 4ehp [52; 53].

MATERIALS AND METHODS

Cell culture and materials

HM1 mouse ES cells derived from OLA/129 genetic background (provided by Dr. Klaus Willecke, University of Bonn GE) were maintained under feeder free conditions in GMEM medium containing $5x10^5$U mouse recombinant leukemia inhibitory factor (LIF; PAA). All other cell lines were purchased from ATCC. MCF7 human breast cancer cells, 4T1 mouse breast cancer cells and H1299 human non-small-cell lung cancer cells were maintained in RPMI medium. U2OS human sarcoma cells were kept in DMEM. All media contained 10% FBS and 25 U/ml penicillin, and 25 µg/ml streptomycin. All cell lines, including stable shRNA expressing derivatives, were confirmed to be mycoplasma-free using the Mycosensor kit from Stratagene. For stable gene silencing, cells were transduced using lentiviral TRC shRNA vectors at MOI 1 (LentiExpressTM; Sigma-Aldrich; Dr. Rob Hoeben and Mr Martijn Rabelink, University Hospital, Leiden NL) according to the manufacturers' procedures and bulk selected in medium containing 2.5 µg/ml puromycin. Control vector expressed shRNA targeting TurboGFP.

Genotoxicants included the DNA cross-linkers cisplatin (Cis-PtCl2(NH3)2) (provided by the Pharmacy unit of University Hospital, Leiden NL) and mitomycin C (Sigma), as well as the inhibitors of topoisomerase II-mediated DNA unwinding, doxorubicin (Sigma) and etoposide (Sigma). Oxidative stressor diethyl maleate (DEM), microtubule poison Vincristine, and ER stressor Thapsigaragin were from Sigma. The pan-caspase inhibitor z-Val-Ala-DL-Asp-fluoromethylketone (z-VAD-fmk) was purchased from Bachem, the eif2α dephosphorylation inhibitor salubrinal was from Calbiochem. ATM inhibitor KU-5593 and proteasome inhibitor MG132 was from Tocris Biosciences. Antibodies against p53 and phospho-p53 were purchased from Novacostra and Cell signaling, respectively. Antibodies against tubulin and FLAG were obtained from Sigma. Antibodies against mouse or human 4ehp and eiF4g2 were from Cell signaling. ARIH1 and 53BP1 antibodies were from Novus Biologicals, while γH2AX antibody was from Millipore. Monoclonal antibody against ubiquitin was purchased from Enzo-Biosciences (FK2 clone).

RNAi experiments

siRNAs were purchased from ThermoFisher Scientific. For primary screens, the Dharmacon siGENOME® SMARTpool® siRNA Library- Mouse Ubiquitin Conjugation Subsets 1 (G-015610), 2 (G-015620) and 3 (G-015630) were used. For Deubiquitination and SUMOylation-screens customized siRNA libraries (Table S1) were used. For deconvolution confirmation screens, customized libraries containing 4 individual siRNAs targeting each selected mRNA were used. GFP, Lamin A/C, and RISC free control siRNAs were used according to MIARE guidelines. Kif11 siRNA was used as transfection efficiency control. The siRNA screens were performed on a Biomek FX (Beckman Coulter) liquid handling system. 50 nM siRNA was transfected in 96 well plates using Dharmafect1 transfection reagent (ThermoFisher Scientific). The medium

was refreshed every 24 h and cells were exposed to indicated compounds or vehicle controls 64 h post-transfection for 24 h. Primary screens were done in duplicate and deconvolution screens were done in quadruplicate. As readout, a cell viability assay using ATPlite 1Step kit (Perkin Elmer) was performed according to the manufacturer's instructions followed by luminescence measurement using a plate reader.

RNAi screen data analysis

As a quality control Z'-factors were determined for each plate, using Lamin A/C as a negative control and p53 as a positive control. To rank the results, Z-scores were calculated using as a reference i) the mean of all test samples in the primary screen and ii) the mean of the negative control samples in the secondary deconvolution screen (in order to prevent bias due to pre-enrichment of hits) [57].Hit determination was done using Z-scores with a cut off value of 1.5 below or above the reference and p-value lower than 0.05. Enrichment of canonical pathways and formation of p53/ ubiquitination signaling network was performed using MetaCore™ data-mining software.

Apoptosis and cell cycle analysis

ES cells were exposed to vehicle or cisplatin for 8 h for cell cycle analysis or 24 h for apoptosis analysis. MCF7 cells were exposed for 24 h for cell cycle analysis. Floating and attached cells were pooled and fixed in 80 % ethanol overnight. Cells were stained using PBS EDTA containing 7.5 mM propidium iodine and 40 mg/ml RNAseA and measured by flow cytometry (FACSCanto II; Becton Dickinson). The amount of cells in the different cell cycle fractions or in sub G0/G1 for apoptotic cells was calculated using BD FACSDiva software. Alternatively, apoptosis was determined using live imaging of Annexin V labeling, as described previously [58].

Clonogenic survival assay

U2OS cells (250 cells/plate) expressing different shRNAs were seeded in triplicate in 9 cm plates. The following day, cells were treated with a dose range of genotoxic agents (γ-irradiation, cisplatin, UVC). After a recovery period of 10 days, surviving cells were fixed, stained and colonies were counted to assay each cell-line's clonogenic potential.

Western blot analysis

Extracts were prepared in TSE containing protein inhibitor cocktail and separated by SDS-PAGE on polyacrylamide gels, transferred to PVDF membranes, and membranes were blocked using 5% BSA. Following incubation with primary and secondary antibodies signal was detected using a Typhoon™ 9400 from GE Healthcare.

Immunofluorescence

U2OS cells were seeded on glass coverslips and allowed to grow for two days. Subsequently, they were treated with cisplatin or irradiated with 0.5 Gy and fixed using 2% formaldehyde for 20 min at the indicated timepoints. After washing extensively

and rehydrating in PBS, post-fixation extraction took place by incubating with 0.25% Triton-X for 5 min. Cells were extensively washed with PBS to remove detergent and then blocked in 5% BSA. Finally coverslips were immunostained with rabbit anti 53BP1 and mouse anti γH2AX, or mouse anti FLAG and rabbit anti eiF4G2 antibodies, followed by counterstaining with DAPI and appropriate secondary fluorescent antibodies.

Cap binding assay

HM1 ES cells, U2OS, and MCF7 breast cancer cells were seeded in 6-well plates at a density of 0.5 million cells/ well. Cells were treated with different concentrations of cisplatin for 4 h (U2OS, MCF7) or 8 h (ES) and proteins were harvested in lysis buffer containing 1 mM phenylmethylsulfonyl fluoride (Cell Signaling). Cap binding proteins were precipitated using 7-methyl-GTP-Sepharose 4B beads (Amersham) as described previously [59]. Precipitated proteins were separated on 12% SDS-PAGE gels and analyzed by immunoblotting for 4ehp (EIF4E2).

Metabolic labeling for detection of translational changes after cisplatin treatment

Click-iT® Metabolic Labeling Reagents for Proteins was purchased from Invitrogen and used according to manufacturers instructions. In short U2OS cells were seeded to 80% confluence in 96 well µclear plates and subsequently treated with 15 µM cisplatin for 2-8 h or with 2 mg/ml cyclohexamide (CHX) for 1 h, or for 2 h with a combination of 15 µM cisplatin and 2.5 µM salubrinal. During the last hour of treatment medium was replaced with methionine-free medium. Subsequently, cells were incubated with azide-labeled methionine analogue for 1 h and fixed for 15 min in 4 % formaldehyde and stained according to manufacturers protocol. DAPI was used as counterstain and images were acquired using a BD-pathway imaging system. Image analysis was performed using BD Attovision software.

Coimmunoprecipitation

U2OS cells, expressing different shRNAs, were transiently transfected with FLAG-tagged wild type 4ehp or Lys[K121/130/134/222R]-mutant 4ehp cDNAs in absence or presence of pCAGGS-5HA-mISG15 cDNA (provided by Dong-Er Zhang, Scripps Research Institute, La Jolla CA - through Addgene; plasmids 17342, 17353 and 12444) [37] or GFP control plasmid in OptiMEM (Invitrogen), using JetPEI (Polyplus) Transfection. The following day, medium was refreshed and 72 h post transfection cells were lysed in FLAG-lysisbuffer (50mM Tris-HCl pH 7.4, 150 mM NaCl, 1mM EDTA, 0.5% NP-40, 0.5% Triton-X, 1 mM PMSF, supplemented with complete protease inhibitor cocktail (Roche)). After 30 min incubation on ice, lysates were diluted 5 x with FLAG-dilution buffer (50 mM Tris-HCl pH7.4, 150 mM NaCl, 1 mM EDTA, 1 mM PMSF, supplemented with complete protease inhibitor cocktail) and incubated with prewashed M2-FLAG magnetic beads (Sigma) for 3 h. Subsequently, beads were washed 3 x for 5 min with FLAG-dilution buffer and lysed in Laemmli-SDS-sample buffer.

qPCR

RNA was extracted using RNeasy Plus Mini Kit from Qiagen. cDNA was made from 50 ng total RNA with RevertAid H minus First strand cDNA synthesis kit (Fermentas) and real-time qPCR was subsequently performed in triplicate using SYBR green PCR (Applied Biosystems) on a 7900HT fast real-time PCR system (Applied Biosystems). The following qPCR primer sets were used: GAPDH, forward (fw) AGCCACATCGCTCAGACACC reverse (rev) ACCCGTTGACTCCGACCTT; ARIH1 (fw) TCATGCCTCTACCCAAGCCTT (rev) ACCAAACCCACAGCAACACA. Data were collected and analyzed using SDS2.3 software (Applied Biosystems). Relative mRNA levels after correction for GAPDH control mRNA were expressed using 2^(-ΔΔCt) method.

ACKNOWLEDGEMENTS

We are grateful to Dr. Rob Hoeben, Dr. Dong-Er Zhang, Mr. Martijn Rabelink, and Dr. Klaus Willecke for generously providing cells and reagents. This work was supported by the Netherlands Genomics Initiative /Netherlands Organization for Scientific Research (NWO): nr 050-060-510.

REFERENCES

1. Jackson, S. P. & Bartek, J. (2009). The DNA-damage response in human biology and disease. Nature 461, 1071-8.

2. Ciccia, A. & Elledge, S. J. (2010). The DNA damage response: making it safe to play with knives. Mol Cell 40, 179-204.

3. Matsuoka, S., Ballif, B. A., Smogorzewska, A., McDonald, E. R., 3rd, Hurov, K. E., Luo, J., Bakalarski, C. E., Zhao, Z., Solimini, N., Lerenthal, Y., Shiloh, Y., Gygi, S. P. & Elledge, S. J. (2007). ATM and ATR substrate analysis reveals extensive protein networks responsive to DNA damage. Science 316, 1160-6.

4. Reinhardt, H. C. & Yaffe, M. B. (2009). Kinases that control the cell cycle in response to DNA damage: Chk1, Chk2, and MK2. Curr Opin Cell Biol 21, 245-55.

5. Bergink, S. & Jentsch, S. (2009). Principles of ubiquitin and SUMO modifications in DNA repair. Nature 458, 461-7.

6. Komander, D. (2009). The emerging complexity of protein ubiquitination. Biochem Soc Trans 37, 937-53.

7. Morris, J. R. (2010). More modifiers move on DNA damage. Cancer Res 70, 3861-3.

8. Skaug, B. & Chen, Z. J. (2010). Emerging role of ISG15 in antiviral immunity. Cell 143, 187-90.

9. Staub, O. (2004). Ubiquitylation and isgylation: overlapping enzymatic cascades do the job. Sci STKE 2004, pe43.

10. Brooks, C. L. & Gu, W. (2006). p53 ubiquitination: Mdm2 and beyond. Mol Cell 21, 307-15.

11. Crosetto, N., Bienko, M. & Dikic, I. (2006). Ubiquitin hubs in oncogenic networks. Mol Cancer Res 4, 899-904.

12. Wood, L. M., Sankar, S., Reed, R. E., Haas, A. L., Liu, L. F., McKinnon, P. & Desai, S. D. (2011). A novel role for ATM in regulating proteasome-mediated protein degradation through suppression of the ISG15 conjugation pathway. PLoS One 6, e16422.

13. Kerscher, O., Felberbaum, R. & Hochstrasser, M. (2006). Modification of proteins by ubiquitin and ubiquitin-like proteins. Annu Rev Cell Dev Biol 22, 159-80.

14. Nagy, V. & Dikic, I. (2010). Ubiquitin ligase complexes: from substrate selectivity to conjugational specificity. Biol Chem 391, 163-9.

15. Wenzel, D. M., Lissounov, A., Brzovic, P. S. & Klevit, R. E. (2011). UBCH7 reactivity profile reveals parkin and HHARI to be RING/HECT hybrids. Nature 474, 105-8.

16. Reinhardt, H. C., Cannell, I. G., Morandell, S. & Yaffe, M. B. (2011). Is post-transcriptional stabilization, splicing and translation of selective mRNAs a key to the DNA damage response? Cell Cycle 10, 23-7.

17. Braunstein, S., Badura, M. L., Xi, Q., Formenti, S. C. & Schneider, R. J. (2009). Regulation of protein synthesis by ionizing radiation. Mol Cell Biol 29, 5645-56.

18. Connolly, E., Braunstein, S., Formenti, S. & Schneider, R. J. (2006). Hypoxia inhibits protein synthesis through a 4E-BP1 and elongation factor 2 kinase pathway controlled by mTOR and uncoupled in breast cancer cells. Mol Cell Biol 26, 3955-65.

19. Silvera, D., Formenti, S. C. & Schneider, R. J. (2010). Translational control in cancer. Nat Rev Cancer 10, 254-66.

20. Kong, J. & Lasko, P. (2012). Translational control in cellular and developmental processes. Nat Rev Genet 13, 383-94.

21. Gingras, A. C., Raught, B. & Sonenberg, N. (1999). eIF4 initiation factors: effectors of mRNA recruitment to ribosomes and regulators of translation.

Annu Rev Biochem 68, 913-63.

22. Gross, J. D., Moerke, N. J., von der Haar, T., Lugovskoy, A. A., Sachs, A. B., McCarthy, J. E. & Wagner, G. (2003). Ribosome loading onto the mRNA cap is driven by conformational coupling between eIF4G and eIF4E. Cell 115, 739-50.

23. Moudry, P., Lukas, C., Macurek, L., Hanzlikova, H., Hodny, Z., Lukas, J. & Bartek, J. (2012). Ubiquitin-activating enzyme UBA1 is required for cellular response to DNA damage. Cell Cycle 11, 1573-82.

24. Zhang, X., Berger, F. G., Yang, J. & Lu, X. (2011). USP4 inhibits p53 through deubiquitinating and stabilizing ARF-BP1. EMBO J 30, 2177-89.

25. Meulmeester, E., Maurice, M. M., Boutell, C., Teunisse, A. F., Ovaa, H., Abraham, T. E., Dirks, R. W. & Jochemsen, A. G. (2005). Loss of HAUSP-mediated deubiquitination contributes to DNA damage-induced destabilization of Hdmx and Hdm2. Mol Cell 18, 565-76.

26. Dayal, S., Sparks, A., Jacob, J., Allende-Vega, N., Lane, D. P. & Saville, M. K. (2009). Suppression of the deubiquitinating enzyme USP5 causes the accumulation of unanchored polyubiquitin and the activation of p53. J Biol Chem 284, 5030-41.

27. Fu, X., Yucer, N., Liu, S., Li, M., Yi, P., Mu, J. J., Yang, T., Chu, J., Jung, S. Y., O'Malley, B. W., Gu, W., Qin, J. & Wang, Y. (2010). RFWD3-Mdm2 ubiquitin ligase complex positively regulates p53 stability in response to DNA damage. Proc Natl Acad Sci U S A 107, 4579-84.

28. Yang, X., Li, H., Zhou, Z., Wang, W. H., Deng, A., Andrisani, O. & Liu, X. (2009). Plk1-mediated phosphorylation of Topors regulates p53 stability. J Biol Chem 284, 18588-92.

29. Lin, J. R., Zeman, M. K., Chen, J. Y., Yee, M. C. & Cimprich, K. A. (2011). SHPRH and HLTF act in a damage-specific manner to coordinate different forms of postreplication repair and prevent mutagenesis. Mol Cell 42, 237-49.

30. Jung, Y. S., Hakem, A., Hakem, R. & Chen, X. (2011). Pirh2 E3 ubiquitin ligase monoubiquitinates DNA polymerase eta to suppress translesion DNA synthesis. Mol Cell Biol 31, 3997-4006.

31. Roy, R., Chun, J. & Powell, S. N. (2012). BRCA1 and BRCA2: different roles in a common pathway of genome protection. Nat Rev Cancer 12, 68-78.

32. Liu, S., Chu, J., Yucer, N., Leng, M., Wang, S. Y., Chen, B. P., Hittelman, W. N. & Wang, Y. (2011). RING finger and WD repeat domain 3 (RFWD3) associates with replication protein A (RPA) and facilitates RPA-mediated DNA damage response. J Biol Chem 286, 22314-22.

33. Tan, N. G., Ardley, H. C., Rose, S. A., Leek, J. P., Markham, A. F. & Robinson, P. A. (2000). Characterisation of the human and mouse orthologues of the Drosophila ariadne gene. Cytogenet Cell Genet 90, 242-5.

34. Li, Z., Musich, P. R. & Zou, Y. (2011). Differential DNA damage responses in p53 proficient and deficient cells: cisplatin-induced nuclear import of XPA is independent of ATR checkpoint in p53-deficient lung cancer cells. Int J Biochem Mol Biol 2, 138-145.

35. Kumar, V., Sabatini, D., Pandey, P., Gingras, A. C., Majumder, P. K., Kumar, M., Yuan, Z. M., Carmichael, G., Weichselbaum, R., Sonenberg, N., Kufe, D. & Kharbanda, S. (2000). Regulation of the rapamycin and FKBP-target 1/mammalian target of rapamycin and cap-dependent initiation of translation by the c-Abl protein-tyrosine kinase. J Biol Chem 275, 10779-87.

36. Tan, N. G., Ardley, H. C., Scott, G. B., Rose, S. A., Markham, A. F. & Robinson, P. A. (2003). Human homologue of ariadne promotes the ubiquitylation of translation initiation factor 4E homologous protein, 4EHP. FEBS Lett 554, 501-4.

37. Okumura, F., Zou, W. & Zhang, D. E. (2007). ISG15 modification of the eIF4E cognate 4EHP enhances cap structure-binding activity of 4EHP. Genes Dev 21, 255-60.

38. Yi, Z., Yi, T. & Wu, Z. (2006). cDNA cloning, characterization and expression analysis of DTX2, a human WWE and RING-finger gene, in human embryos. DNA Seq 17, 175-80.

39. Matsumoto, A., Onoyama, I., Sunabori, T., Kageyama, R., Okano, H. & Nakayama, K. I. (2011). Fbxw7-dependent degradation of Notch is required for control of "stemness" and neuronal-glial differentiation in neural stem cells. J Biol Chem 286, 13754-64.

40. Welcker, M. & Clurman, B. E. (2008). FBW7 ubiquitin ligase: a tumour suppressor at the crossroads of cell division, growth and differentiation. Nat Rev Cancer 8, 83-93.

41. Yamamoto, H., Koga, H., Katoh, Y., Takahashi, S., Nakayama, K. & Shin, H. W. (2010). Functional cross-talk between Rab14 and Rab4 through a dual effector, RUFY1/Rabip4. Mol Biol Cell 21, 2746-55.

42. Balut, C. M., Loch, C. M. & Devor, D. C. (2011). Role of ubiquitylation and USP8-dependent deubiquitylation in the endocytosis and lysosomal targeting of plasma membrane KCa3.1. FASEB J 25, 3938-48.

43. Kuroda, T. S., Fukuda, M., Ariga, H. & Mikoshiba, K. (2002). The Slp homology domain of synaptotagmin-like proteins 1-4 and Slac2 functions as a novel Rab27A binding domain. J Biol Chem 277, 9212-8.

44. Larsen, D. H., Poinsignon, C., Gudjonsson, T., Dinant, C., Payne, M. R., Hari, F. J., Rendtlew Danielsen, J. M., Menard, P., Sand, J. C., Stucki, M., Lukas, C., Bartek, J., Andersen, J. S. & Lukas, J. (2010). The chromatin-remodeling factor CHD4 coordinates signaling and repair after DNA damage. J Cell Biol 190, 731-40.

45. Nakayama, E. E. & Shioda, T. (2010). Anti-retroviral activity of TRIM5 alpha. Rev Med Virol 20, 77-92.

46. Okumura, F., Matsuzaki, M., Nakatsukasa, K. & Kamura, T. (2012). The Role of Elongin BC-Containing Ubiquitin Ligases. Front Oncol 2, 10.

47. Cencic, R., Hall, D. R., Robert, F., Du, Y., Min, J., Li, L., Qui, M., Lewis, I., Kurtkaya, S., Dingledine, R., Fu, H., Kozakov, D., Vajda, S. & Pelletier, J. (2011). Reversing chemoresistance by small molecule inhibition of the translation initiation complex eIF4F. Proc Natl Acad Sci U S A 108, 1046-51.

48. Shamji, A. F., Nghiem, P. & Schreiber, S. L. (2003). Integration of growth factor and nutrient signaling: implications for cancer biology. Mol Cell 12, 271-80.

49. Clarke, R., Cook, K. L., Hu, R., Facey, C. O., Tavassoly, I., Schwartz, J. L., Baumann, W. T., Tyson, J. J., Xuan, J., Wang, Y., Warri, A. & Shajahan, A. N. (2012). Endoplasmic reticulum stress, the unfolded protein response, autophagy, and the integrated regulation of breast cancer cell fate. Cancer Res 72, 1321-31.

50. Morita, M., Ler, L. W., Fabian, M. R., Siddiqui, N., Mullin, M., Henderson, V. C., Alain, T., Fonseca, B. D., Karashchuk, G., Bennett, C. F., Kabuta, T., Higashi, S., Larsson, O., Topisirovic, I., Smith, R. J., Gingras, A. C. & Sonenberg, N. (2012). A Novel 4EHP-GIGYF2 Translational Repressor Complex Is Essential for Mammalian Development. Mol Cell Biol 32, 3585-93.

51. Sonenberg, N. & Gingras, A. C. (1998). The mRNA 5' cap-binding protein eIF4E and control of cell growth. Curr Opin Cell Biol 10, 268-75.

52. Cho, P. F., Poulin, F., Cho-Park, Y. A., Cho-Park, I. B., Chicoine, J. D., Lasko, P. & Sonenberg, N. (2005). A new paradigm for translational control: inhibition via 5'-3' mRNA tethering by Bicoid and the eIF4E cognate 4EHP. Cell 121, 411-23.

53. Lasko, P. (2011). Posttranscriptional regulation in Drosophila oocytes and early embryos. Wiley Interdiscip Rev RNA 2, 408-16.

54. Gingras, A. C., Kennedy, S. G., O'Leary, M. A., Sonenberg, N. & Hay, N. (1998). 4E-BP1, a repressor of mRNA translation, is phosphorylated and

inactivated by the Akt(PKB) signaling pathway. Genes Dev 12, 502-13.

55. Joshi, B., Cameron, A. & Jagus, R. (2004). Characterization of mammalian eIF4E-family members. Eur J Biochem 271, 2189-203.

56. Wiseman, R. L. & Balch, W. E. (2005). A new pharmacology--drugging stressed folding pathways. Trends Mol Med 11, 347-50.

57. Birmingham, A., Selfors, L. M., Forster, T., Wrobel, D., Kennedy, C. J., Shanks, E., Santoyo-Lopez, J., Dunican, D. J., Long, A., Kelleher, D., Smith, Q., Beijersbergen, R. L., Ghazal, P. & Shamu, C. E. (2009). Statistical methods for analysis of high-throughput RNA interference screens. Nat Methods 6, 569-75.

58. Puigvert, J. C., de Bont, H., van de Water, B. & Danen, E. H. (2010). High-throughput live cell imaging of apoptosis. Curr Protoc Cell Biol Chapter 18, Unit 18 10 1-13.

59. Moody, C. A., Scott, R. S., Amirghahari, N., Nathan, C. O., Young, L. S., Dawson, C. W. & Sixbey, J. W. (2005). Modulation of the cell growth regulator mTOR by Epstein-Barr virus-encoded LMP2A. J Virol 79, 5499-506.

.

SUPPLEMENTARY MATERIALS

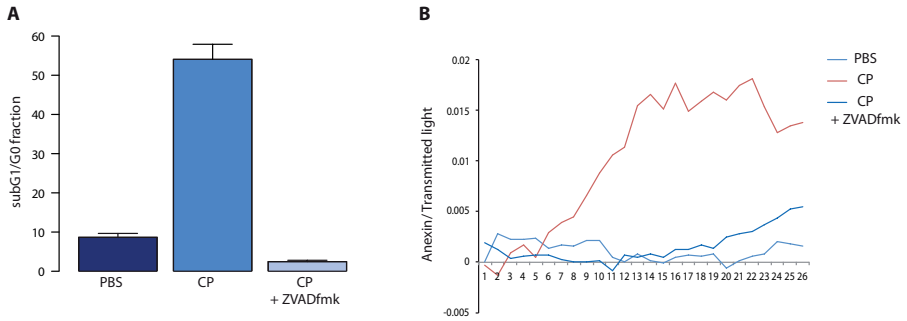

Figure S1. Caspase-dependent apoptosis in ES cells treated with cisplatin. (A) SubG1/G0 apoptotic fraction in HM1 ES cells treated with 7.5 μM CP for 24 h and prevention by 100 μM pan-Caspase inhibitor ZVADfmk. (B) Real time imaging of fluorescently labeled Annexin V binding [58] shows accumulation of apoptotic ES cells during treatment with 7.5 μM CP and prevention by 100 μM ZVADfmk. Ratio [AnexinV signal: total cell area] is shown.

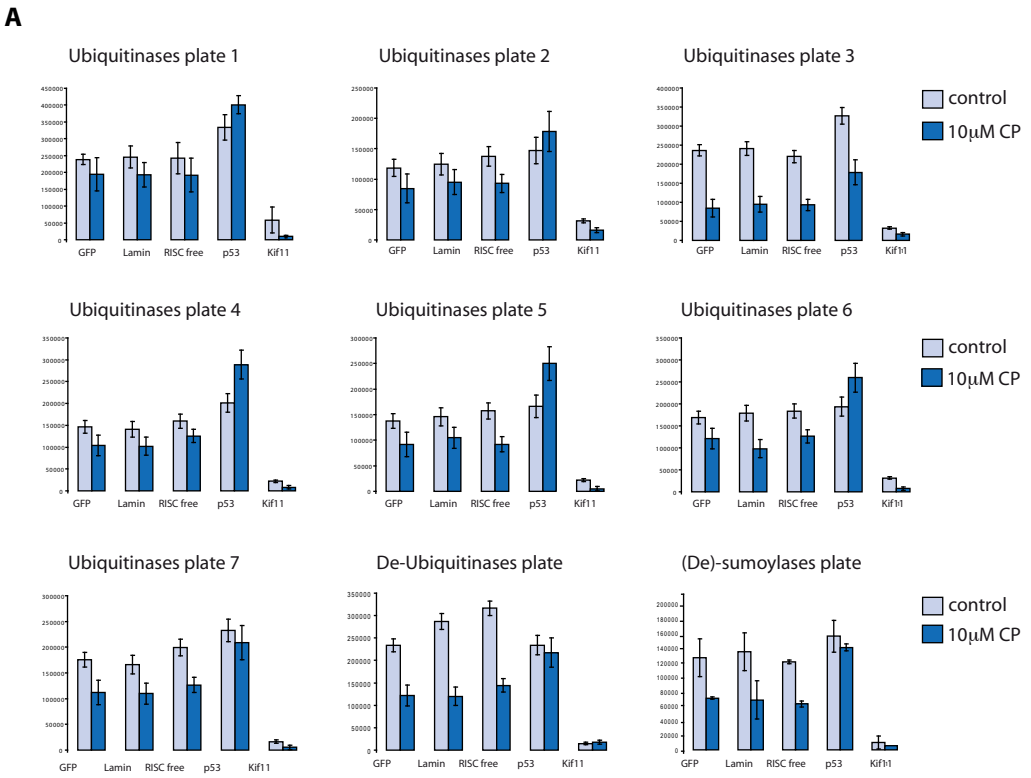

B

$$Z' \text{ - factor} = 1 - \frac{3 \times (s_p + s_n)}{|m_p - m_n|} = 0.45$$

Figure S2. Ubiquitination/sumoylation screen transfection controls. (A) ATP-lite read out for indicated set of control siRNAs in each Smartpool library plate. Bars show average and standard deviation of two control and two 10 μM CP-treated plates. (B) Average Z´-factor calculated for siLamin and sip53.

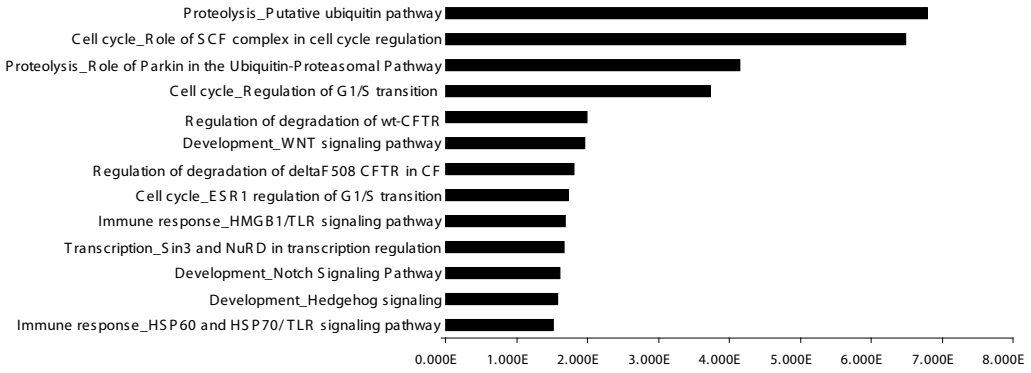

Figure S3. Pathway analysis for Ubiquitination/sumoylation screen hits. Enriched canonical pathways predicted from 27 confirmed screen hits using Metacore bioinformatics software, ranked by log p-value.

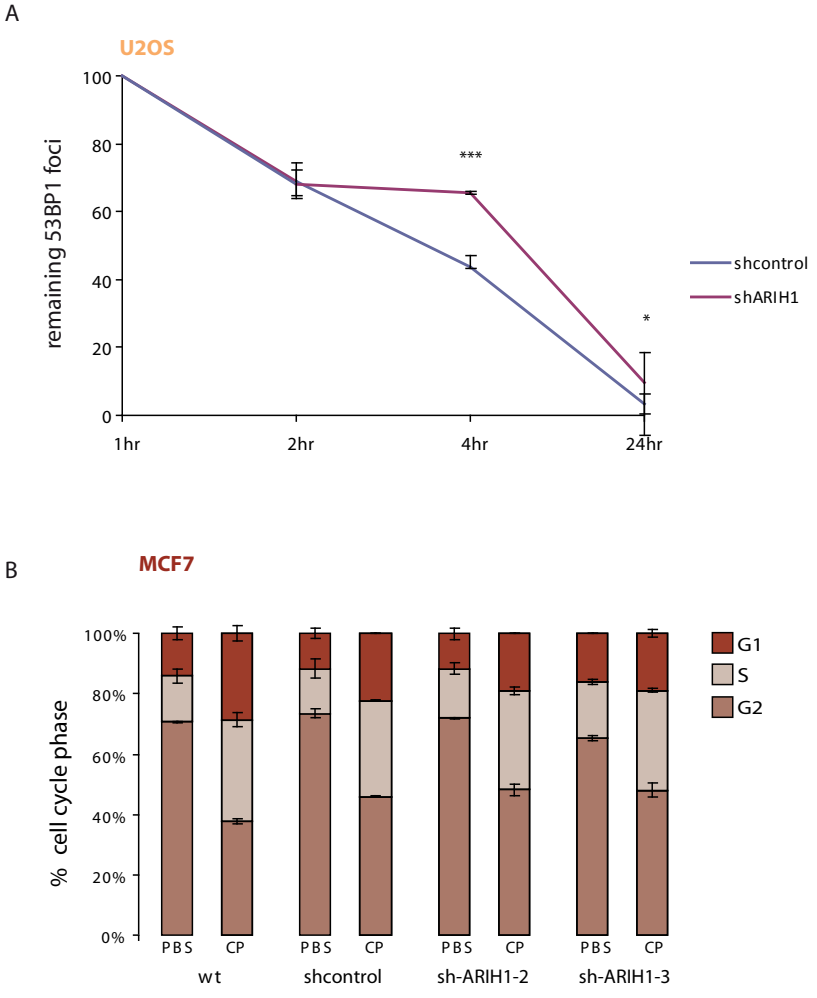

Figure S4. DNA damage-induced foci formation and cell cycle profiles for MCF7 shARIH1 cell lines. (A) Quantification of remaining 53BP1 foci after γ–irradiation in shcontrol and shARIH1 U2OS cells 1 2, 4, and 24 h after irradiation. (B) Quantification of cell cycle profiles in wt, shcontrol and shARIH1-2, -3 MCF7 cell lines after treatment with 10 μM CP for 24 h.

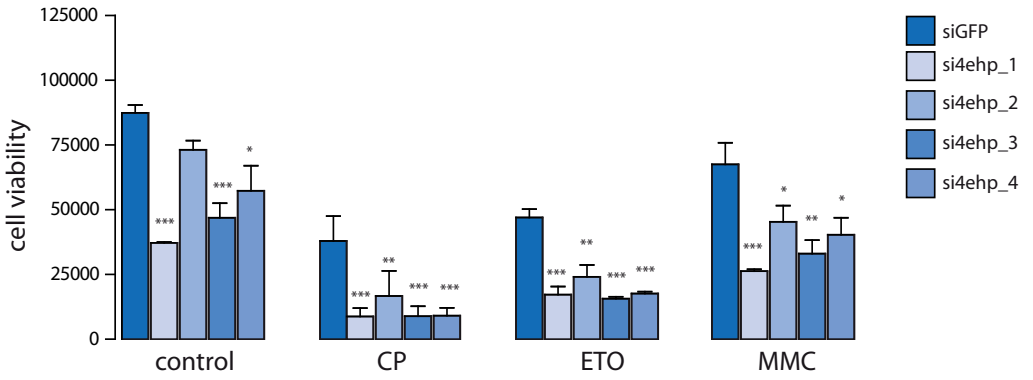

Figure S5. Single siRNA sequences targeting 4ehp sensitize ES cells. Cell viability assay in presence of siRNA targeting GFP, p53, Kif11 and 4 individual sequences targeting 4ehp after control treatment, treatment with 10 μM CP, 150 nm ETO or 10 μg/μl MMC.

Gene Symbol	Gene Id	Accession Number
MJD	110616	NM_029705
E030022H21RIK	217218	NM_001098837
DUB-1A	381944	NM_201409
DUB2	13532	NM_010089
BAP1	104416	NM_027088
C130067A03RIK	320713	NM_177239
TNFAIP3	21929	NM_009397
1810057B09RIK	223527	NM_175009
HIST2H2BE	319190	NM_178214
DXIMX46E	54644	NM_138604
C6.1A	210766	NM_145956
CYLD	74256	NM_173369
FBXO7	69754	NM_153195
FBXO8	50753	NM_015791
E130307M08RIK	68047	NM_026530
1300006C06RIK	74158	NM_028792
1110007C05RIK	66124	NM_025368
OTUB1	107260	NM_134150
4930586I02RIK	68149	NM_026580
4933428L19RIK	71198	XM_991213
D8ERTD69E	73945	NM_001081164
2600013N14RIK	72201	NM_152812
USP1	230484	NM_146144
USP2	53376	NM_198091
USP3	235441	NM_144937
USP4	22258	NM_011678
USP5	22225	NM_013700
USP7	252870	NM_001003918
USP8	84092	NM_019729
USP9X	22284	NM_009481
USP9Y	107868	NM_148943
USP10	22224	NM_009462
USP11	236733	NM_145628
USP12	22217	NM_011669
USP13	72607	NM_001013024
USP14	59025	NM_001038589
USP15	14479	NM_027604
USP16	74112	NM_024258
Usp17	436004	NM_001033494
USP18	24110	NM_011909
USP19	71472	NM_027804
USP20	74270	NM_028846
USP21	30941	NM_013919
USP22	216825	NM_001004143
Usp24	329908	XM_915524
USP25	30940	NM_013918
USP26	83563	NM_031388
USP28	235323	NM_175482
USP29	57775	NM_021323
USP30	100756	NM_001033202
6330567E21RIK	76179	XM_992065
USP32	237898	NM_001029934
USP33	170822	NM_001076676
LOC244144	244144	XM_886523
Usp36	72344	XM_916680
4932415L06RIK	319651	NM_176972
USP38	74841	NM_027554
USP39	28035	NM_138592
USP40	227334	NM_001033291
Usp42	76800	NM_029749
USP43	216835	NM_173754
E430004F17	327799	NM_183199
4930550B20RIK	77593	NM_152825
2410018I08RIK	69727	NM_177561
USP47	74996	NM_133758
USP48	170707	NM_130879
C330046L10RIK	224836	NM_198421
4930511O11RIK	75083	NM_029163
LOC635253	635253	NM_001137547
USP52	103135	NM_133992
AA939927	99526	NM_133857
USP54	78787	NM_030180
UBR1	22222	NM_009461
C330046L10RIK	224836	NM_198421
4930511O11RIK	75083	NM_029163
LOC635253	635253	NM_001137547
USP52	103135	NM_133992
AA939927	99526	NM_133857
USP54	78787	NM_030180
UBR1	22222	NM_009461
UCHL1	22223	NM_011670
UCHL3	50933	NM_016723
UCHL5	56207	NM_019562
UFD1L	22230	NM_011672
UBE4B	63958	NM_022022
COPS5	26754	NM_013715
PLP2	18824	NM_019755

Customized Deubiquitinases Library

Gene Symbol	Gene Id	Accession Number
UBLE1B	50995	NM_016682
Ube2i	22196	NM_011665
MDM2	17246	NM_010786
D11BWG0280E	52915	NM_028601
BC065120	328365	NM_183208
PIAS1	56469	NM_019663
MIZ1	17344	NM_008602
PIAS3	229615	NM_018812
PIAS4	59004	NM_021501
RANBP2	19386	NM_011240
CBX4	12418	NM_007625
2510027N19RIK	67711	NM_026330
TOPORS	106021	NM_134097
RNF110	22658	NM_009545
SENP1	223870	NM_144851
SENP2	75826	NM_029457
SENP3	80886	NM_030702
SENP5	320213	NM_177103
SENP6	215351	NM_146003
2810413I22RIK	66315	NM_001003973
SENP8	71599	NM_027838

Customized (De)-Sumoylases Library

Table S1. Custom siRNA libraries for Deubiquitinases and (De)-Sumoylases. Indicated are gene symbols, Entrez IDs and Accession numbers.

gene symbol	Z-score	p-value
RBX1	-3.49229	0.000239
FBXO6A	-2.96913	0.001493
SYTL4	-2.69639	0.003505
RCHY1	-2.68571	0.003619
RNF166	-2.67699	0.003714
Rfwd3	-2.51751	0.005909
UBE1X	-2.28613	0.011123
TCE1	-2.25446	0.012084
ARIH1	-2.16801	0.015079
FBXW7	-2.11149	0.017365
TOPORS	-2.11004	0.017428
BARD1	-2.05953	0.019722
C730024G19RIK	-2.05522	0.019929
LOC380928	-2.0437	0.020492
LOC381621	-2.02454	0.021458
USP8	-2.02454	0.021458
UBE2D3	-2.02396	0.021487
CHD4	-1.93042	0.026778
BRCA1	-1.85984	0.031454
PHF15	-1.85	0.032157
TRIM21	-1.80426	0.035595
SHPRH	-1.75546	0.03959
MKRN2	-1.73969	0.040957
USP4	-1.73969	0.040957
A530081L18RIK	-1.70491	0.044106
DXIMX46E	-1.70491	0.044106
FBXW5	-1.68291	0.046196
USP5	-1.45575	0.07273
USP7	-1.37068	0.085238
Usp42	1.637496	0.050763
FBXO17	1.650206	0.04945
ASB3	1.656369	0.048824
1110002E23RIK	1.708269	0.043793
LOC668173	1.728961	0.041908
6330567E21RIK	1.728961	0.041908
Trim61	1.750478	0.040018
FBXO34L	1.804707	0.03556
MGRN1	1.934613	0.026519
4933428L19RIK	1.934613	0.026519
DTX2	1.986825	0.023471
AL033326	2.010687	0.022179
USP54	2.078665	0.018824
ZNRF2	2.153452	0.015642
LNX2	2.196345	0.014034
CUL4A	2.21634	0.013334
RNF110	2.29063	0.010992
USP22	2.29063	0.010992
CUL1	2.479363	0.006581
CDC34	2.994131	0.001376
E430004F17	3.097247	0.000977

Table S2. Hits from primary ubiquitination screens. Indicating gene symbols, Z-scores and p-values.

gene symbol	gene ID	Accession number	Function	validation
USP4 *	22258	NM_011678	DUB	2 out of 4
USP7 *	252870	NM_001003918	DUB	3 out of 4
USP8	84092	NM_019729	DUB	4 out of 4
DXIMX46E	54644	NM_138604	DUB	2 out of 4
E430004F17	327799	NM_183199	DUB	2 out of 4
USP5 *	22225	NM_013700	DUB	3 out of 4
RUFY1	216724	NM_172557	no known UB-function	2 out of 4
RCHY1 *	68098	NM_026557	E3	2 out of 4
Rfwd3 *	234736	NM_146218	E3	4 out of 4
4930470D19RIK	67610	NM_026274	no known UB-function	4 out of 4
ARIH1	23806	NM_019927	E3	4 out of 4
UBE1X	22201	NM_009457	E1	4 out of 4
SYTL4	94121	NM_013757	no known UB-function	3 out of 4
CHD4	107932	NM_145979	no known UB-function	3 out of 4
FBXW7	50754	NM_080428	E3	2 out of 4
LOC381621		XM_355579	no known UB-function	2 out of 4
UBE2D3	66105	NM_025356	E2	4 out of 4
DTX2	74198	NM_023742	E3	2 out of 4
ZNRF2	387524	NM_199143	E3	2 out of 4
RBX1	9978	NM_019712	E3	4 out of 4
TCE1	79043	NM_027141	no known UB-function	2 out of 4
TOPORS *	106021	NM_134097	E3	2 out of 4
C730024G19RIK	232566	XM_132975	no known UB-function	3 out of 4
BRCA1	NM_009764	NM_009764	E3	3 out of 4
TRIM21	20821	NM_009277	E3	4 out of 4
SHPRH	268281	NM_172937	E3	2 out of 4
AL033326*	24105	NM_019705	E3	3 out of 4
Fbxo7	69754	NM_153195	E3	3 out of 4

Table S3. Hits from secondary deconvolution-ubiquitination screens. Indicated are gene symbols, Entrez IDs, Accession numbers, ubiquitination function and validation status. Effect on p53 is pointed to by *, sensitizing siRNAs in green; protecting siRNAs in red